

# Experiment Measurement of the Dry Density Variations and Shear Stress with the Different Depth Variations

Thy Truc Doan

Dept. of Technology and Engineering, Kien Giang University, VietNam

## \*Corresponding Author

Thy Truc Doan, Department. of Technology and Engineering, Kien Giang University, VietNam.

Submitted: 2023, Mar 09; Accepted: 2023, Apr 07; Published: 2023, May 09

**Citation:** Thy, T., D. (2023). Experiment Measurement of the Dry Density Variations and Shear Stress with the Different Depth Variations. *Envi Scie Res Rev*, 6(2), 447-459.

## Abstract

Evaluation of the dry density variations and shear stress with the different depth variations were shown clearly with the particular process. Results show the Dry unit weight (density) increases gradually with the increase of different depths. The biggest dry density was obtained at 1.582 g/cm<sup>3</sup> at 18.3m depth of boreholes (“HK1, 2, and 3”); whereas the lowest value was obtained at 0.74 g/cm<sup>3</sup> at 4.3m depth. On the other hand, the dry density changed with the constant loading process. The biggest dry density is 1.954 g/cm<sup>3</sup> at 18.3m depth and the lowest value is 1.482 g/cm<sup>3</sup> at 8.3m depth (before loading); The biggest value is 2.074 g/cm<sup>3</sup> at 18.3m depth and the lowest value is 1.621 g/cm<sup>3</sup> at 8.3m depth (after loading). Moreover, shear stress was measured carefully at different depths. At the Clay layer, the lowest value is  $\tau_1$  with 0.052 kG/cm<sup>2</sup> at 4.8m depth; whereas the biggest is  $\tau_3$  with 1.750 kG/cm<sup>2</sup> at 39.6m depth. The biggest value is  $\tau_2$  with 1.276 kG/cm<sup>2</sup> at 17.8m depth. At the Sand layer, the lowest value is  $\tau_1$  with 0.586 kG/cm<sup>2</sup> at 29.8m depth; whereas the biggest is  $\tau_3$  with 1.750 kG/cm<sup>2</sup> at 39.6m depth and  $\tau_2$  with 1.21 kG/cm<sup>2</sup> at 36.0m depth.

**Keywords:** Dry Unit Weight (Density); Shear Stress; Constant Loading; Variations of Depths

## 1. Introduction

Research on soils in New Zealand and Japan presented the Maximum dry density test to quantify pumice content in natural soils and consideration of the other bound. Results presented the maximum dry density values with the maximum amount of crushing under the 14 kPa surcharge. And the pumice contents of the NP sands which is the reason for the relative breakage of materials during the modified maximum dry density test [1]. Moreover, the cyclic wetting and drying (CWD) under constant volume (CV) conditions and constant stress (CS) caused a reduction in swell pressure while at having almost no impact on  $k_{sat}$ . The relationship between maximum dry density and California Bearing Ratio (CBR) coefficient of soil located in California. Results of some equations are presented clearly as the value of  $R^2$  is 0.962 [2,3]. Three of the shear tests at constant shear stress and dry density of unsaturation soil. Results described the increasing both the dry density and overburden pressure, as well as decreasing both the water intensity [4].

In addition, the samples were dried in the 20°C room temperature condition, the outside of the surface of the sample was cemented and crystallized by the xanthan gum biopolymer; whereas the

inside of the surface is full of moisture and weak cross-linked by the solution. In contrast, the shear strength decreases as water content increase on the surface [5]. The dry density and structure complexity of soil operated at the same time. Result presented with the fractal tortuosity increases whereas fractal dimensions are constant as consideration of the increasing of the dry density [6]. With Chiba soil described particularly of both the air-entry value and the residual suction of drying SWCC. This is the reason for increasing of the dry density of sandy soil; whereas the area of the surface of drying and wetting SWCCs (i.e., hysteresis) decreases [7].

Research on Viscoelasticity and shear resistance at the microscale of naturally structured and homogenized subtropical soils under undefined and defined normal stress conditions. Results presented a higher shear resistance at the end of recoverable deformation (LVR),  $\tau_{LVR}$ , as well as a higher maximum shear resistance,  $\tau_{max}$  [8]. Using the fiber contents to simulate the peak shear strength of these fiber-reinforced expansive soils are different: when the contents of GF and PF are 0.3% and 0.5%. [9]. However, the higher shear resistance parameters with increasing density are explained mainly by increased contact and friction between soil particles [10].

With the confining pressure is over 100 kPa, which results in a dry density is 11.2 g/cm<sup>3</sup> and 12.7 g/cm<sup>3</sup> changed with the increase of deviator stress (kPa) and axial strain [11]. On the other hand, the maximum particle size results in the maximum of shear strength. And the dry density can be obtained in the lowest values as fine contents are high. [12]. In contrast, the dry unit weight of soils decreases as water contents and P-wave velocities of compacted soils increase [13].

One estimation for the dry unit weight by the model of the multi-layer perceptron (MLP) neural networks and general linear model (GLM). Results presented values of the dry unit weight predictions range between 0.47 and 0.99, 0.80 and 0.99 for GLM and MLP models, respectively [14]. A mixing was method used to credit the coefficient 0.9 times the shear strength as consideration of the actual scale SRM on site [15]. With particle diameter D50 and the void ratio are constant. Results presented that a  $G_{max}$  value decreases as the  $C_u$  value increases during the effective confining stress is constant [16]. Moreover, research on the increasing of fine-size fraction; results determined the drained residual strength decreases; whereas the increase in the shear displacement. And grain crushing and fine particles accumulated respectively [17].

However, the dry density obtained at 45kN/m<sup>3</sup> and 0.94 kN/m<sup>3</sup>, the effects of wetting and desiccation shall be obtained by samples P of 321.860454 kPa, W1 by 46.75611 kPa, W2 by 56.6899 kPa, 43,48429 kPa by W3, 65,56742 kPa by W4 by size, W5 by W3 by 37,42705 kPa, W4 by W6 by 32,04,885 kPa by W7, 35.8667 kPa by W8 and 28.588823 kPa by W9 by samples [18]. Experiments in UCS presented clearly the cement content used carefully as consideration of the specific dry mass. But the porosity can't be obtained as respectively, and the maximum values of  $q_u = 3523$  kPa [19]. On the other hand, the increase in the natural soil of COV from 10 to 100%, resulted in the shear strength value of 150.7<sup>2</sup>kN/m<sup>2</sup>; whereas the increase in SI values  $e$  from -1.18 to - 0.823, - 1.07 to - 0.739 and - 0.959 to - 0.654 for BSL, WAS and BSH, in that order [20].

A FORTRAN program was used to generate a safety index (SI) for shear strength values in the range of coefficient of variation (COV) of 10–100%. Results presented a strong interaction between the shear strength values and the soil parameters (Locust bean waste ash, LBWA; Cohesion, CO; Friction angle, FA; Plasticity index, PI; Maximum dry density, MDD; Optimum moisture content, OMC; Percentage fine, PF; Cation exchange capacity, CEC; Specific gravity, G<sub>s</sub> and Compact effort, CE) [21]. Results on evaluation of treated and untreated soil, presented remarkable values about the treated soil is 0.45 MPa whereas the untreated soil is [22].

Using the sensors for measurement of the relationship between the different soil dry bulk densities and observed time. Results described soil moisture to penetrate from soil surface till 25 cm is around 10 mins and 57 mins when density is maintained at 1.1 gm/cc and 1.3 gm/cc, respectively. And the SMSMSP output changes only by 2.7 % when the ambient temperature varies from 20 °C

to 60 °C [23]. The regression model shows good estimates of pre-compression stress for a number of structured soils considering dry bulk density and AD/BD ratio at a matric potential of 6 kPa [24]. Soil is easy to deform as they located on the surface of the crust. And the size of soil particles and the highest drying stress increased after drying stress increased [25].

In addition, the value of soils amended with aqueous <sup>137</sup>Cs, and the drying and wetting cycles' impact on Cs; resulted in an extractable <sup>137</sup>Cs fraction of the water which was very low (< 1%) and decreased over time; whereas the detection limit in soils amended with solid organic sources of <sup>137</sup>Cs [26]. Evaluation of the relationships between the G<sup>0</sup> value and the DA value, which resulted in the difference of the isotropic and anisotropic stress states during undrained cyclic loading as the different void ratios [27]. The compacted specimens obtained a dry density of 1.55 g/cm<sup>3</sup> and water content of 27.5% of the undisturbed lateritic clay. And the microstructure of the specimen is more homogeneous, combined with most sizes of soil pores smaller than 10 μm [28]. Research results show shear stress  $\tau$  versus shear displacement  $\Delta l$  with different dry densities for deep reconstituted soils.

And the shear strength versus normal stress  $\sigma$  for different dry densities with a water content of 20% and the best-fitted lines. The shear strength increases as the dry density increases, whereas shear strength decreases sharply when the dry density is higher than 1.72 g/cm<sup>3</sup> and the corresponding density 2.06 g/cm<sup>3</sup> [29]. The DEM model simulation presented the interlocking effect of gravel to the shear strength, and the increase of weak soil-gravel contact with GC would be limited when GC exceeds 40%. And the stronger the shear performance of the mixture [30].

The experiment of the SWCC presented the relationship between the van Genuchten parameters and the dry density of compacted bentonites. Results demonstrated that the increase of the dry density corresponds to an exponential decrease in  $\alpha$  and a linear increase in  $n$  [31].

## 2. Materials, machines, and Experiments

### 2.1 Experiment in the laboratory

Research on the My Thai Canal Bridge, Hon Dat town, Kien Giang province, in Viet Nam which is used for measurement in the laboratory and the Field by the Viet Nam Standard [32-34]. Measurement in the laboratory has been done step by step carefully to obtain the best results. Soil with no salt content; Pure water; Density flask (capacity less than 100 cm<sup>3</sup>); weight; Porcelain mortar and pestle; Sieve (hole diameter 2 millimeters); electric stove; Oven; vacuum flask; Hydrometer; conical hopper; Heat stabilizer; aluminum can with cap; and so on.

### 2.2 Experiments in the Field

The research location was done at the three boreholes "HK" which include "HK1, HK2, HK3" at latitude 10<sup>0</sup>09'35" North and 104<sup>0</sup>58'39" East of the My Thai Canal Bridge, Hon Dat town, Kien Giang province, in Viet Nam. Field surveying has been done

carefully by the Viet Nam Standards, which include the detailed process, survey, drilling, and sample protection until doing the experiment with the purpose to obtain the best results. Field experiments were implemented by the Standard Penetration Test “SPT” at depths from +2.0m to -40.0m. The Ground is divided into

small seven layers (Layer 1a; Layer 1; Layer 2a; Layer 2; Layer 2b; Layer 3 and Layer 4). In this research, the ground is divided into two big layers, which include a “Clay layer” from 0.0m to 27.0m depths; and a “Sand layer” from 27.0m to 40.m depths (see Figures 1 and 2).

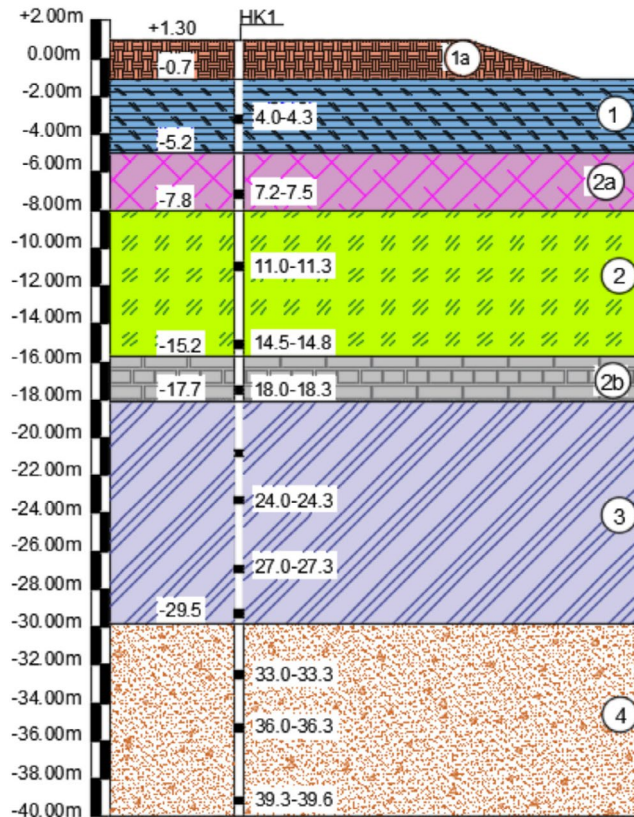


Figure 1a: Stratigraphic cross-section (borehole “HK1”)



Figure 1b: Research location (Source: <https://earth.google.com/>)

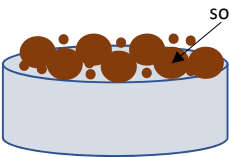
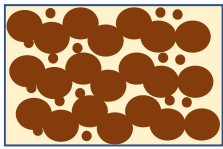
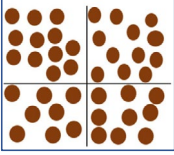

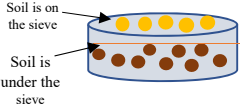
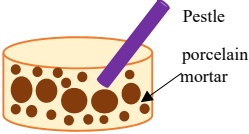

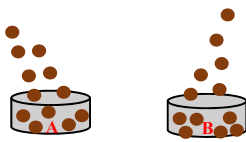
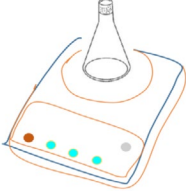
| Layer | Thickness (m)       | Soil properties      | Water content (humidity) W (%) | Unit weight above the groundwater level $\gamma_w$ (g/cm <sup>3</sup> ) | Porosity n (%) | Saturation G (%) | Plasticity index PI | Internal friction angle $\phi_0$ | Cohesion C (kg/cm <sup>2</sup> ) |
|-------|---------------------|----------------------|--------------------------------|---|----------------|------------------|---------------------|----------------------------------|----------------------------------|
| 1     | From -0.7 to -5.2   | Silt mixed clay      | 92.24                          | 1.401   | 71.40          | 94.15            | 24.72               | 2013'                            | 0.045                            |
| 2a    | From -5.2 to -7.8   | Clay; semi-hard      | 28.35                          | 1.881   | 46.26          | 89.77            | 21.72               | 14037'                           | 0.409                            |
| 2     | From -7.8 to -15.2  | Clay; semi-hard      | 26.15                          | 1.903   | 44.69          | 88.31            | 21.34               | 15058'                           | 0.455                            |
| 2b    | From -15.2 to -17.7 | Clay; semi-hard      | 21.72                          | 1.961   | 40.95          | 85.43            | 21.68               | 18055'                           | 0.585                            |
| 3     | From -17.7 to -29.5 | Semi-clay, semi-hard | 21.99                          | 1.917   | 41.56          | 83.16            | 14.91               | 16051'                           | 0.337                            |
| 4     | From -29.5 to -39.6 | Sand, semi-tightness | 18.66                          | 1.864   | 41.22          | 71.11            | -                   | 28024'                           | 0.057                            |

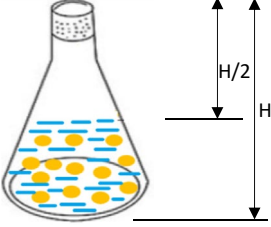
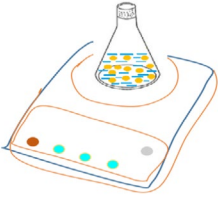

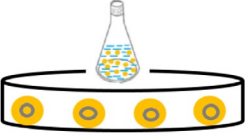
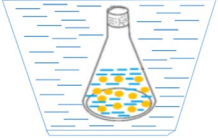
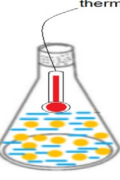
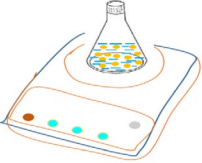

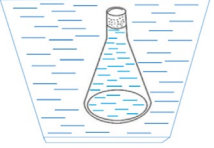
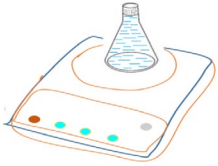
**Table 1: Soil characteristics with the medium values “TCVN 4195:2012”**

### 3. Method and results

#### 3.1 Dry unit weight (dry density)

##### 3.1.1 Implementation process

|  |  |   |
|--|--|---|
|    |    |    |
| <p>Step 1: Soil is put with air drying outside by wind (with 400 grams)</p>  | <p>Step 2: Soil is crushed by hand</p>   | <p>Step 3: Soil is divided into 4 same parts</p>  |
|  <p>Step 4: Soil is selected from step 3, and use 100 grams of the total of two symmetrical parts and mix together.</p> |  <p>Step 5: Soil is sieved (with 2 millimeters of sieve diameter)</p>   |  <p>Step 6: Soil is on the sieve which is crushed by the pestle and porcelain mortar until no soil on the sieve.</p> |
|  <p>Step 7: Soil is on the sieve which is poured into the flask (15 grams)</p>  |  <p>Step 8: Soil is under the sieve which is put into two cups “A and B” to determine the degree of hygroscopicity (10 grams)</p> |  <p>Step 9: Weigh the flask (no suspension); Volume of the flask is 100 cm<sup>3</sup></p>                            |

|  |  |  |
|--|--|--|
|  <p>Step 10: Pour the pure water to reach the center of the flask which contains soil (H/2).</p>  |  <p>Step 11: Weigh the flask that contains soil and water (or it is called “suspension”).</p>   |  <p>Step 12: Keep the flask on hand and shake evenly from 10 to 15 minutes until the suspension is even.</p>   |
|  <p>Step 13: The flask is put on the stove to boil. After finishing the boiling process, and then do the cooling of the suspension.</p> |  <p>Step 14: The flask is put in the container which contains water to cool. After finished cooling, remove the flask out of the container, and do a temperature measurement.</p>   |  <p>Step 15: A thermometer is used to measure the temperature of the suspensions (results show exactly 0.5°C). Every 15 minutes measurement and recording results.</p> |
|  <p>Step 16: Weight the flask which contains suspensions again</p>   |  <p>Step 17: Pour out the suspensions from the flask outside, and clean the flask completely.</p>  |  <p>Step 18: Pure water is poured into the flask (no suspension), and put in the container which contains water to cool</p>   |
|  <p>Step 19: Weight the flask which contains water after the finish of the cooling process</p>  | <p>* <b>Note:</b></p> <ul style="list-style-type: none"> <li>+ Results should be shown with an accuracy of 0.01 gram/cm<sup>3</sup>.</li> <li>+ The suspension temperature should be at 20°C.</li> <li>+ Sand is boiled within 30 minutes. It is necessary to determine the degree of hygroscopicity before doing the following experiments.</li> <li>+ Clay is boiled within 1 hour.</li> </ul> |  |

### 3.2.2 The related equations for determination of the Dry unit weight (dry density) with Depths

The absolute dry soil mass ( $m_0$ ) in the flask is calculated by the formulas below:

$$m_0 = \frac{m_1}{1+0.01w_h} \quad (1)$$

Whereas,  $m_1$  is the mass of soil sample which is at air drying outside by wind, gram (g)  $w_h$  is the content of the hygroscopicity of soil, (%).

Unit weight (density) of soil ( $\rho$ ) is calculated by the formulas below:

$$\rho = \frac{m_0}{m_0+m_3-m_2} \times \rho_n \quad (2)$$

Whereas,  $m_0$  is the absolute drying mass in the flask, (gram, g)  
 $m_2$  is the mass of the flask which contains suspension (pure water and soil), (gram, g)  
 $m_3$  is the mass of the flask which contains full water, (gram, g)  
 $\rho_n$  is the density of water at a temperature which is done in the experiment, (gram/cm<sup>3</sup>).

### 3.3 Results

#### 3.3.1 The relationship between the Dry Unit Weight variations and Depths

From the analysis results above, the calculation was done one by one at different depths. Results were shown in figure 1 such as: Dry unit weight changed at the different depths and depend on types of soil diameter. The minimum value is 0.74 gram/cm<sup>3</sup> at 4.3m depth; compared with the maximum value of 1.626 gram/cm<sup>3</sup>

at 17.8m depth. The medium value at the center of the layer is 1.44 gram/cm<sup>3</sup> (from 0.0m to 27.0m depth); whereas this value increased gradually to 1.57 gram/cm<sup>3</sup> of the layer 1 “Clay layer” (from 27.0m to 40.0m depth). (see Figure 2).

From the above results (see figure 3), it is easy to see that the biggest value of dry density obtained of 1.597 g/cm<sup>3</sup>; 1.582 g/cm<sup>3</sup>; 1.580 g/cm<sup>3</sup> at 18.3m depth of boreholes “HK1, 2, and 3”). On the contrary, the lowest dry density was obtained at 0.74 g/cm<sup>3</sup> and 0.718 g/cm<sup>3</sup> at 4.3m depth of boreholes “HK1, 2”; whereas at borehole 3 “HK3” is up to 1.549 g/cm<sup>3</sup> at 11.3m depth. On the other hand, with figure 4 (see figure 4), it is easy to see that the biggest value of dry density obtained of 1.582 g/cm<sup>3</sup> at 18.3m depth of boreholes “HK1, 2, and 3”); whereas the lowest dry density was obtained at 0.74 g/cm<sup>3</sup> at 4.3m depth.

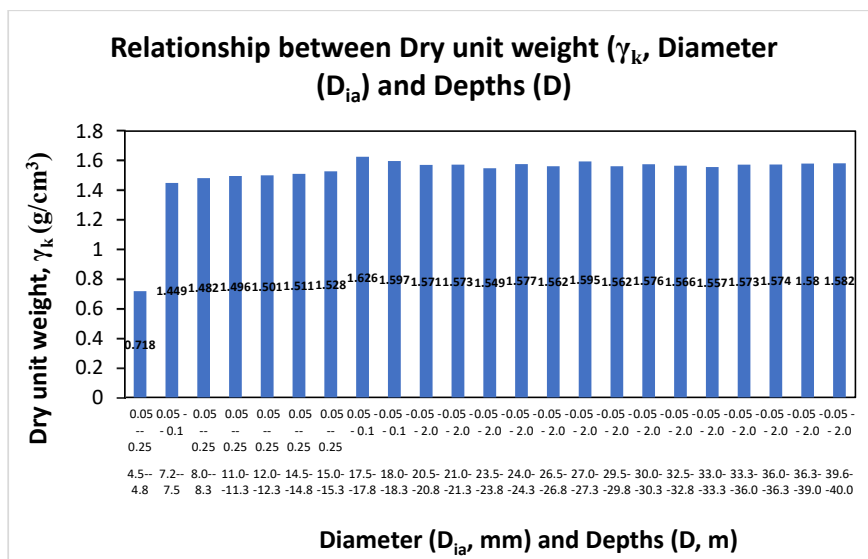


Figure 2: Relationship between Dry unit weight (gram/cm<sup>3</sup>), Diameter (mm), and Depths (m)

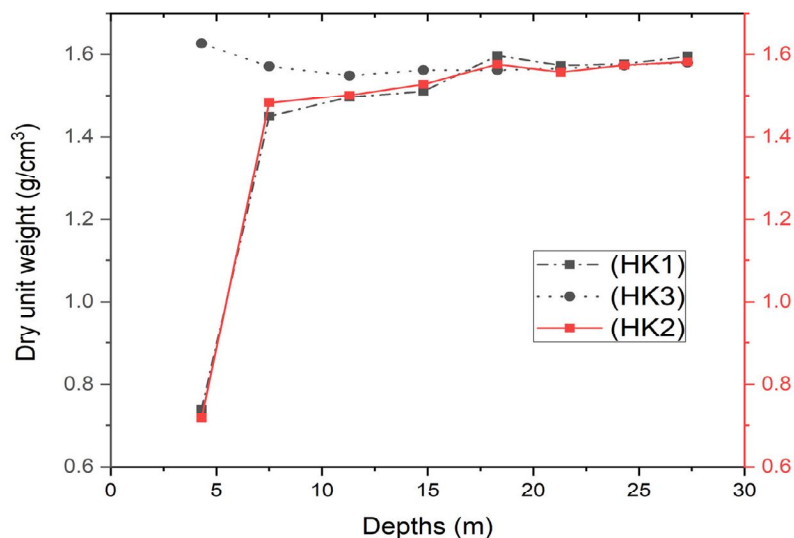
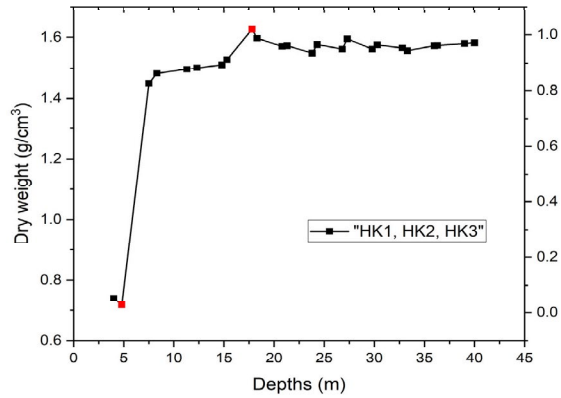


Figure 3: Dry unit weight (gram/cm<sup>3</sup>) variations with Depths (m) from 0.0m to 27.0m

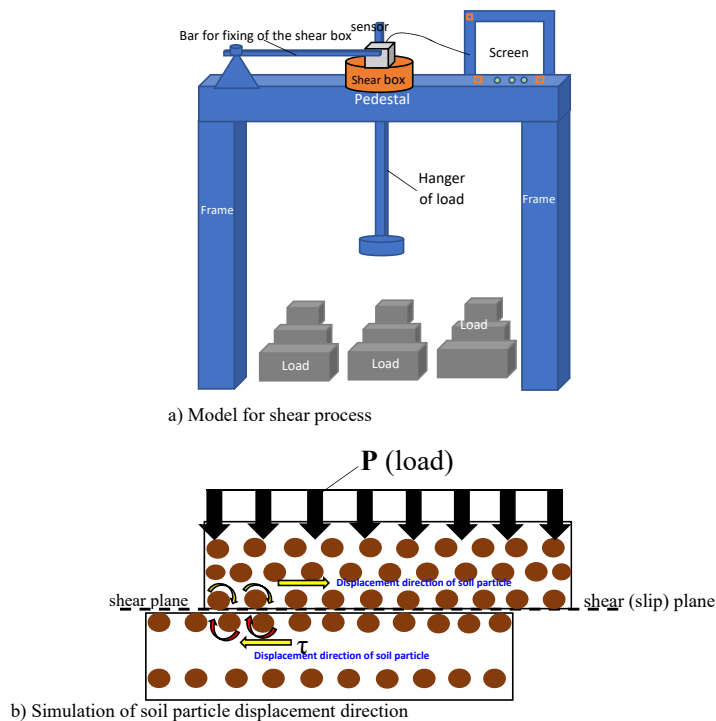


**Figure 4:** Dry unit weight ( $\gamma_k$ , gram/cm<sup>3</sup>) variations with Depths (D, m) from 0.0m to 40.0m

### 3.3.2 The relationship between Dry unit weight (kN/m<sup>3</sup>) variations and Constant Loading P (kPa)

| Descriptions                        | Notations   | Values             | Unit                                 |
|-------------------------------------|-------------|--------------------|--------------------------------------|
| Speed                               | $S_p$       | 0.0001 ~ 900       | °/minute ~ °/minute                  |
| Maximum stress                      | $S_{max}$   | 1000               | kPa                                  |
| Normal stress                       | $S_{norma}$ | 1000               | kPa                                  |
| Weight of machine                   | $W_m$       | 0.1                | Tone (T)                             |
| Area of machine                     | $A_r$       | 380                | Square millimeter (mm <sup>2</sup> ) |
| Height of machine                   | $H_m$       | C1400              | millimeter (mm)                      |
| The outside diameter of the machine | $D_o$       | 100                | millimeter (mm)                      |
| Inside diameter of the machine      | $D_i$       | 70                 | millimeter (mm)                      |
| Thickness of machine                | Th          | 5                  | millimeter (mm)                      |
| Electricity source                  | $ES_r$      | 90 ~ 240 and 50/60 | Volts/ Hz                            |

**Table 2. Specification of the Shear machine “VJTech”**



**Figure 5:** Simulation of shear process

The samples are saturated completely after 24 hours. For all of the samples with size 60x60mm which are put in a Shear machine for time for the cutting process is 0.005mm/ minute. Loading is constant value  $P = 0.5\text{kg/cm}^2$ . When the shear process begins (see figure 5), soil particles connect together with the purpose prevent shear force. And when the shear force of the machine is rather than the linked force of soil particles together, so the destruction process will be done on the surface of soil particles together.

During this process, soil particles will be slipped on the flat together, which creates friction forces. These friction forces have the same directions, which are located in the horizontal direction. After this slip process has been finished, the soil particle surface

will be destructed clearly. Results have been shown particularly in figure 6 (see figure 6).

From the result of figure 6, it is easy to see that at 12.0m; 21.0m, and 25.0m depths, dry unite weight (density) increases by  $2.024\text{ g/cm}^3$ ;  $1.697\text{ g/cm}^3$ ; and  $1.706\text{ g/cm}^3$ . Moreover, these values decrease gradually with 8.0m; 15m; and 21.0m depths with  $1.482\text{ g/cm}^3$ ;  $1.642\text{ g/cm}^3$ , and  $1.577\text{ g/cm}^3$ . After loading is a little changing as compared with before loading. The biggest value is  $1.954\text{ g/cm}^3$  at 18.3m depth (before loading); the lowest value is  $1.482\text{ g/cm}^3$  at 8.3m depth (before loading); The biggest value is  $2.074\text{ g/cm}^3$  at 18.3m depth (after loading); the lowest value is  $1.621\text{ g/cm}^3$  at 8.3m depth (before loading).

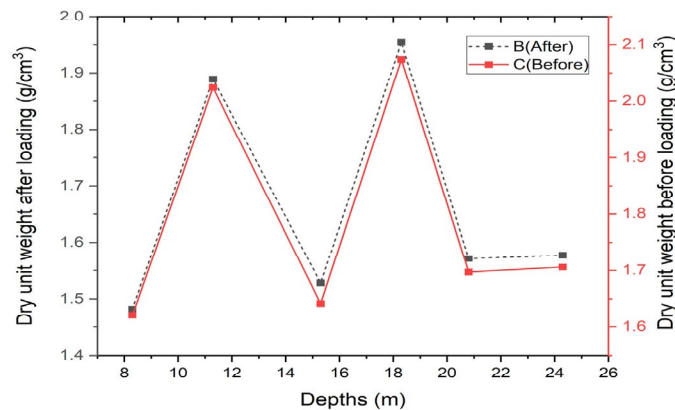


Figure 6: Dry unit weight ( $\text{gram/cm}^3$ ) and Constant load ( $P = 0.5\text{kg/cm}^2$ )

### 3.2.3 The relationship between Shear stress variations and Depths

The Shear stress variation experiments were done at three boreholes “HK1, 2, and 3”. Loading is designed in this process which is shown with the different values corresponding to different loading levels such as:  $0.25\text{ kg/cm}^2$ ;  $0.5\text{ kg/cm}^2$ ;  $1.0\text{ kg/cm}^2$ ;  $1.25\text{ kg/cm}^2$ ;  $1.5\text{ kg/cm}^2$ ;  $2.0\text{ kg/cm}^2$ ;  $3.0\text{ kg/cm}^2$ ;  $4.0\text{ kg/cm}^2$ . Shear stress values  $\tau_1$ ,  $\tau_2$ , and  $\tau_3$  were shown with different depths.

From 4.0m to 27.0m Depths of borehole 1 “HK1”, shear stress values  $\tau_1$ ,  $\tau_2$ , and  $\tau_3$  increase with different depths (see figure 6).

The value of the shear stress  $\tau_1$  less changed as compared with values  $\tau_2$ , and  $\tau_3$ . In contrast, shear stress values  $\tau_3$  and  $\tau_2$  are almost equal. On the other hand, from 4.0m to 18.0m depths, shear stress increased with the maximum value of shear stress  $\tau_3$  was obtained at  $1.276\text{ kG/cm}^2$  at 27.0m depth; compared with  $0.06\text{ kG/cm}^2$  of shear stress  $\tau_1$  at 4.3m depth. And the biggest shear stress  $\tau_2$  was obtained at  $1.233\text{ kG/cm}^2$  at 18.3m depth; Moreover, this value decreases gradually and becomes constant as depths continue increasing gradually at 27.0m. It is clear to conclude that shear stress variations increase gradually with different depths.

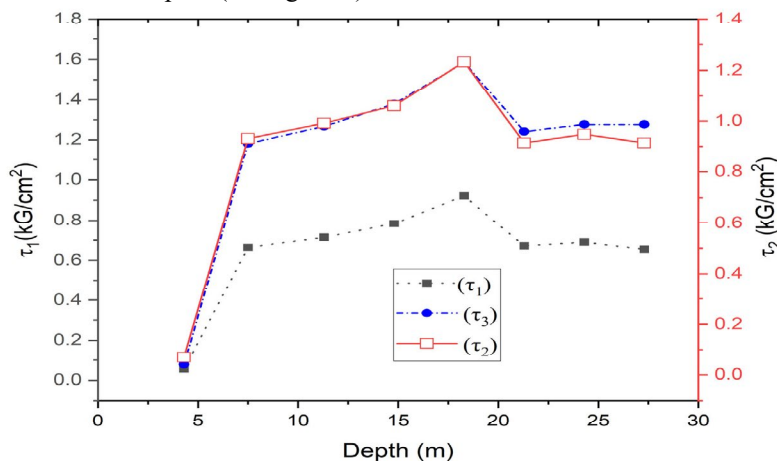
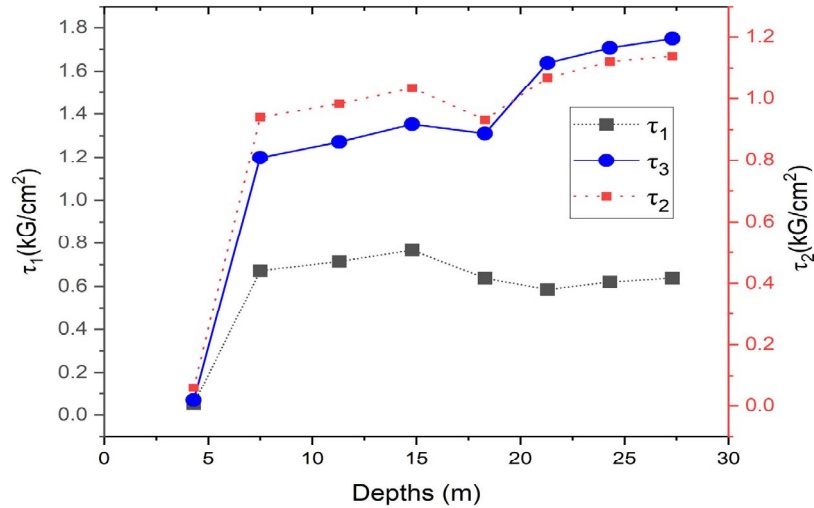


Figure 6: Shear stress variations and Depths of borehole 1 “HK1” (from the depth at the bottom of each layer at 4.0m to 27.0m)



From 4.0m to 27.0m Depths of borehole 2 “HK2”, shear stress  $\tau_1$ ,  $\tau_2$ , and  $\tau_3$  presented increasing gradually with different depths (see figure 7). The shear stress value  $\tau_1$  less change as compared with  $\tau_2$ , and  $\tau_3$ . Moreover, the values of shear stress  $\tau_2$  and  $\tau_3$  change most equally. On the other hand, shear stress  $\tau_3$  was obtained at the biggest value of 1.310 kG/cm<sup>2</sup> at 30.3m depth; whereas less increase with the lowest value  $\tau_1$  of 0.052 kG/cm<sup>2</sup>; and relatively stable  $\tau_2$  with 1.034 kG/cm<sup>2</sup> at 15.3m depths. All these maximum values show at 18.0m depth and the value of shear stress  $\tau_1$

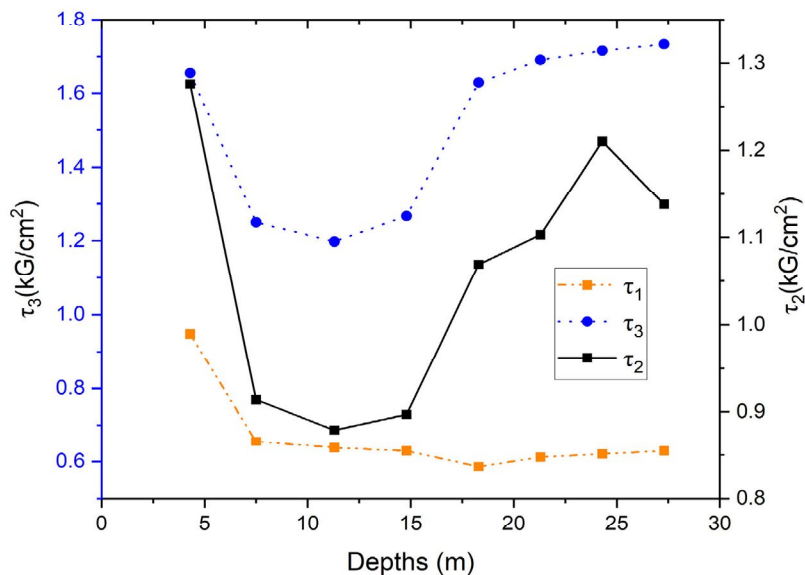
decrease gradually until constant as the increasing up to 27.0m depth of the remaining values. Moreover, from 18.0m to 27.0m depths, shear stress  $\tau_1$  increase gradually and stability, whereas the value of shear stress  $\tau_2$  continues to increase. However, the value  $\tau_2$  fewer increases as compared with  $\tau_3$ . So it is clear that shear stress changed clearly with different depths. The shear stresses increase with different Depths. The clear difference and the biggest value obtained in this result is value  $\tau_3$ .



**Figure 7:** Shear stress variations and Depths of borehole 2 “HK2” (from the depth at the bottom of each layer at 4.0m to 27.0m)

From 4.0m to 27.0m depths, borehole 3 “HK3” presented quite clearly shear stress  $\tau_1$ ,  $\tau_2$ , and  $\tau_3$  increase with depths (see figure 8). The value of shear stress  $\tau_1$  fewer a change of 0.948 kG/cm<sup>2</sup> at 5.0m depth; as compared with values  $\tau_2$ , and  $\tau_3$ . On the contrary, the value of shear stress  $\tau_2$  obtains a maximum value of 1.276 kG/cm<sup>2</sup> at 5.0m depth. And then these values decrease dramatically to 1.267 kG/cm<sup>2</sup> at 7.0m depth and increase gradually from 7.0m

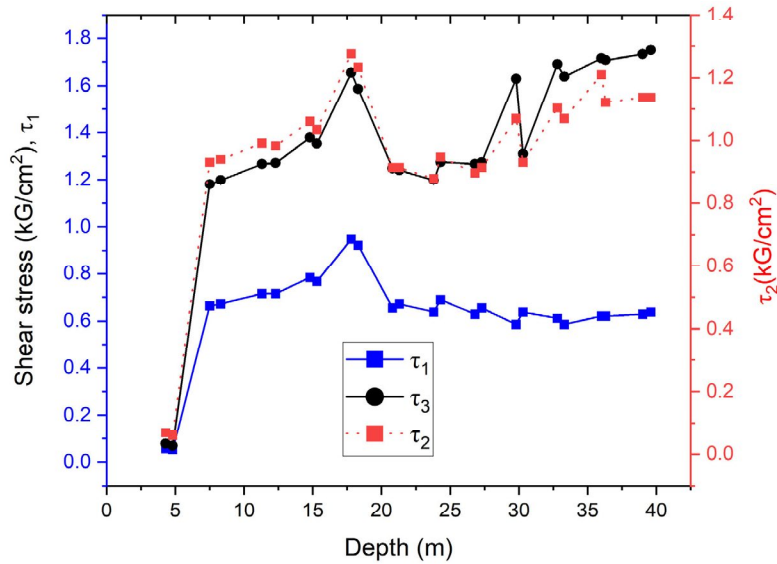
to 15.0m depth. On the contrary, shear stress  $\tau_3$  increase gradually but it fewer changes as compared with value  $\tau_2$ ; In addition, from 15.0m to 27.0m depths, these values increase relatively steadily; whereas the biggest value of shear stress is  $\tau_3$  at 27.0m depth, and the lowest value is  $\tau_1$ . The increasing shear stress is not stable with depths. The clear difference and biggest values are  $\tau_3$ .



**Figure 8:** Shear stress variations and Depths of borehole 3 “HK3” (from the depth at the bottom of each layer at 4.0m to 27.0m)

On the other hand, from 4.0m to 40.0m depths, borehole 3 “HK1,2 and 3” show shear stress values  $\tau_1$ ,  $\tau_2$ , and  $\tau_3$  increase clearly with different depths (see figure 9). Generally, all of the values change with increasing gradually and stabilize with increasing depths. The

lowest value and less change are  $\tau_1$  with  $0.052 \text{ kG/cm}^2$  at 4.8m depth; whereas the biggest and more change values are  $\tau_3$  with  $1.750 \text{ kG/cm}^2$  at 39.6m depth. Finally, the biggest value of stability is  $\tau_2$  with  $1.276 \text{ kG/cm}^2$  at 17.8m depth.

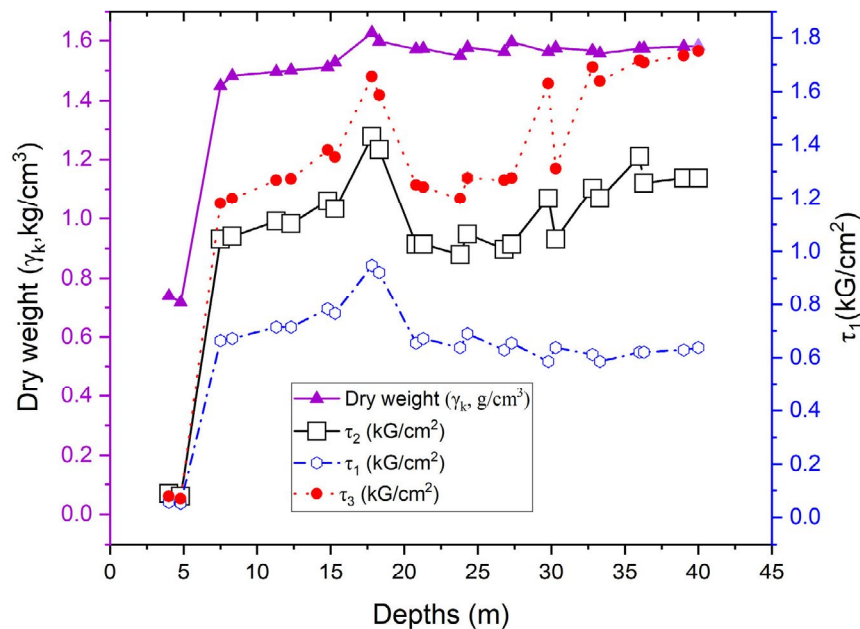


**Figure 9:** Total of Shear Stress with  $\tau_1$ ,  $\tau_2$ ,  $\tau_3$ , (from 0.0m to 40.0m); boreholes “HK1, HK2, HK3”

### 3.2.4 The relationship between Dry unit weight (density) and Shear Stress at Depths (from 0.0m to 40.0m)

The relationship between dry unit weight (density) and shear stress with different depths was presented clearly in figure 10 (see figure 10). From figure 10, it is easy to see that dry density changed relative stability with shear stress  $\tau_1$ , and these values increase gradually with the increasing depths. Moreover, the biggest and

most remarkable values of dry density and three shear stress show clearly of  $1.626 \text{ g/cm}^3$ ;  $0.948 \text{ kG/cm}^2$  ( $\tau_1$ );  $1.276 \text{ kG/cm}^2$  ( $\tau_2$ ); and  $1.655 \text{ kG/cm}^2$  ( $\tau_3$ ) at 18.0m depth; whereas dry density and shear stress  $\tau^1$  change with gradual decrease and stability with the depth increasing. In contrast, the shear stress  $\tau^2$  and  $\tau^3$  continue to increase remarkably. So it is easy to conclude that depths increase and dry density and shear stress increase respectively.



**Figure 10:** Total of Shear Stress ( $\tau$ ) and Dry unit weight ( $\gamma_k$ ) at Depths (D) of the Clay layer with  $\tau_1$ ,  $\tau_2$ ,  $\tau_3$ , (from 0.0m to 40.0m); boreholes “HK1, HK2, HK3”

### 3. Discussion

Research on the change of the dry unit weight (density) has been shown clearly as an analysis of variations with different depths. The medium value of the Clay layer (from 4.0m to 27.0m) obtains 1.44 g/cm<sup>3</sup>. Whereas compared with the layered sand (from 27.0m to 39.6m) up to 1.57 g/cm<sup>3</sup>. The medium value of the total of depths (from 0.0m to 40.0m) obtained 1.491.57 g/cm<sup>3</sup>.

With the constant load  $P = 0.5 \text{ kG/cm}^2$  for the Shear stress determination to determine the shear stress decrease gradually as increasing of depths. Differences between loading before and after loading at three boreholes have been presented particularly.

At borehole 1 “HK1”, the value is 0.135 kG/cm<sup>2</sup>; 0.12 kG/cm<sup>2</sup>; and 1.129 kG/cm<sup>2</sup> at 11.3m; 18.3, and 24.3m depths; whereas compared with the borehole 2 “HK2” value of 0.139 kG/cm<sup>2</sup> and 0.114 kG/cm<sup>2</sup> at 8.3m and 15.3m depth. Finally, the value at borehole 3 “HK3” is up to 0.126 kG/cm<sup>2</sup> at 20.8m depth.

In contrast, when consideration was done at shear stress values  $\tau_1$ ,  $\tau_2$ ,  $\tau_3$  at boreholes “HK1, HK2, and HK3” with a remarkable change in the different depths. The medium values of shear stress  $\tau_1$ ,  $\tau_2$ ,  $\tau_3$  account for 0.63 kG/cm<sup>2</sup>; 0.95 kG/cm<sup>2</sup>; and 1.32 kG/cm<sup>2</sup>.

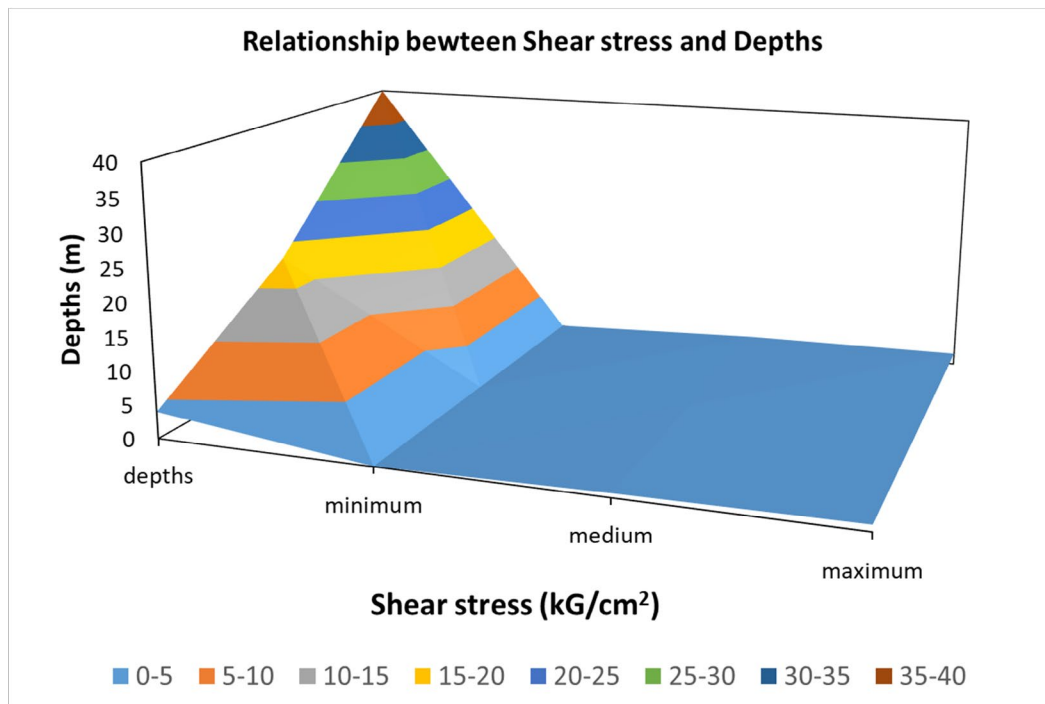


Figure 11: Relationship between Shear stress ( $\tau$ ) and Depths (D)

### 4. Conclusion

Firstly, dry density is evaluated carefully by one particular process, which includes 19 steps. Steps were done carefully to obtain the best results. Dry density increases gradually with the increasing of different depths. This increase is relative stability at boreholes from 8.0m to 40.0m. Moreover, the biggest value of dry density was obtained of 1.582 g/cm<sup>3</sup> at 18.3m depth of boreholes “HK1, 2, and 3”); whereas the lowest dry density was obtained at 0.74 g/cm<sup>3</sup> at 4.3m depth.

Secondly, the dry density changed with the constant loading process. This process was done carefully by the shear machine. The biggest value is 1.954 g/cm<sup>3</sup> at 18.3m depth (before loading); the lowest value is 1.482 g/cm<sup>3</sup> at 8.3m depth (before loading); The biggest value is 2.074 g/cm<sup>3</sup> at 18.3m depth (after loading); the lowest value is 1.621 g/cm<sup>3</sup> at 8.3m depth (after loading).

Thirdly, shear stress was measured carefully one by one of the samples according to one by one of the different depths. At the Clay layer (from 4.0m to 27.0m), the lowest value and less change are  $\tau_1$  with 0.052 kG/cm<sup>2</sup> at 4.8m depth; whereas the biggest and more change values are  $\tau_3$  with 1.750 kG/cm<sup>2</sup> at 39.6m depth. Finally, the biggest value of stability is  $\tau_2$  with 1.276 kG/cm<sup>2</sup> at 17.8m depth. On the other hand, at the Sand layer (from 27.0m to 40.0m), the lowest value and less change are  $\tau_1$  with 0.586 kG/cm<sup>2</sup> at 29.8m depth; whereas the biggest and more change values are  $\tau_3$  with 1.750 kG/cm<sup>2</sup> at 39.6m depth. Finally, the biggest value of stability is  $\tau_2$  with 1.21 kG/cm<sup>2</sup> at 36.0m depth. Finally, the research results of this paper show clearly the process of dry density determination, constant loading, and shear stress with depths. So results will be contributed more remarkable things to geotechnical engineering and researchers in the future.

## List of Notations

| Signs  |   | Detail Describes  | Unit  |
|--|---|---|---|
| <b>The Dry unit weight (dry density) with Depths</b> |   |   |   |
| $m_0$  | = | The absolute dry soil mass  | gram (g)  |
| $m_1$  | = | The mass of soil sample which is air drying outside by the wind       | gram (g)  |
| $w_h$  | = | The content of the hygroscopicity of soil                             | percentage (%)  |
| <b>Unit weight (density) of soil</b>                 |   |   |   |
| $\rho$   | = | Unit weight (density) of soil   | gram/cm <sup>3</sup>                                    |
| $m_0$  | = | The absolute drying mass in the flask                                 | gram (g)  |
| $m_2$  | = | The mass of the flask which contains suspension (pure water and soil) | gram (g)  |
| $m_3$  | = | The mass of the flask which contains full water                       | gram (g)  |
| $\rho_n$   | = | The density of water at a temperature which is done in the experiment | gram/cm <sup>3</sup>                                    |
| $\gamma_k$   | = | Dry unit weight   | gram/cm <sup>3</sup>                                    |
| $D_{ia}$   | = | Diameter of soil particle   | Millimeter (mm)   |
| $D$  | = | Depths  | Meter (m)   |
| $\tau$   | = | Shear Stress  | Kilogram-force/ square centimeter (kG/cm <sup>2</sup> ) |
| $P$  | = | Load  | kPa   |
| <b>*Specification of the Shear machine "VJTech"</b>  |   |   |   |
| $S_p$  | = | Speed   | <sup>o</sup> /minute ~ <sup>o</sup> /minute             |
| $S_{max}$  | = | Maximum stress  | kPa   |
| $S_{norma}$  | = | Nornal stress   | kPa   |
| $W_m$  | = | Weight of machine   | Tone (T)  |
| $A_r$  | = | Area of machine   | Square millimeter (mm <sup>2</sup> )                    |
| $H_m$  | = | Height of machine   | millimeter (mm)   |
| $D_o$  | = | The outside diameter of the machine                                   | millimeter (mm)   |
| $D_i$  | = | Inside diameter of the machine  | millimeter (mm)   |
| $T_h$  | = | Thickness of machine  | millimeter (mm)   |
| $E_{Sr}$   | = | Electricity source  | Volts/ Hz   |

## References

- Asadi, M. S., Orense, R. P., Asadi, M. B., & Pender, M. J. (2019). Maximum dry density test to quantify pumice content in natural soils. *Soils and Foundations*, 59(2), 532-543.
- Abbas, M. F., Shaker, A. A., & Al-Shamrani, M. A. (2023). Hydraulic and volume change behaviors of compacted highly expansive soil under cyclic wetting and drying. *Journal of Rock Mechanics and Geotechnical Engineering*, 15(2), 486-499.
- Bharath, A., Manjunatha, M., Reshma, T. V., & Preethi, S. (2021). Influence and correlation of maximum dry density on soaked & unsoaked CBR of soil. *Materials Today: Proceedings*, 47, 3998-4002.
- Chen, C., Wu, L., Perdjon, M., Huang, X., & Peng, Y. (2019). The drying effect on xanthan gum biopolymer treated sandy soil shear strength. *Construction and Building Materials*, 197, 271-279.
- Chen, Y., Withanage, K. R., Uchimura, T., Mao, W., & Nie, W. (2020). Shear deformation and failure of unsaturated sandy soils in surface layers of slopes during rainwater infiltration. *Measurement*, 149, 107001.
- Du, J., Zhou, A., Shen, S. L., & Bu, Y. (2022). Fractal-based model for maximum penetration distance of grout slurry flowing through soils with different dry densities. *Computers and Geotechnics*, 141, 104526.
- Gallage, C. P. K., & Uchimura, T. (2010). Effects of dry density and grain size distribution on soil-water characteristic curves of sandy soils. *Soils and foundations*, 50(1), 161-172.
- Holthusen, D., Pertile, P., Reichert, J. M., & Horn, R. (2019). Viscoelasticity and shear resistance at the microscale of naturally structured and homogenized subtropical soils under undefined and defined normal stress conditions. *Soil and Tillage Research*, 191, 282-293.
- Holthusen, D., Pertile, P., Awe, G. O., & Reichert, J. M.

- (2020). Soil density and oscillation frequency effects on viscoelasticity and shear resistance of subtropical Oxisols with varying clay content. *Soil and Tillage Research*, 203, 104677.
10. Huang, Z., Sun, H. Y., Dai, Y. M., Hou, P. B., Zhou, W. Z., & Bian, L. L. (2022). A study on the shear strength and dry-wet cracking behaviour of waste fibre-reinforced expansive soil. *Case Studies in Construction Materials*, 16, e01142.
  11. Kawahara, S., & Muro, T. (2006). Effects of dry density and thickness of sandy soil on impact response due to rockfall. *Journal of terramechanics*, 43(3), 329-340.
  12. Kolay, E., & Baser, T. (2014). Estimating of the dry unit weight of compacted soils using general linear model and multi-layer perceptron neural networks. *Applied Soft Computing*, 18, 223-231. DOI: org/10.1016/j.asoc.2014.01.033
  13. Kouakou, N. M., Cuisinier, O., & Masrouri, F. (2020). Estimation of the shear strength of coarse-grained soils with fine particles. *Transportation Geotechnics*, 25, 100-407.
  14. Kim, B. S., Park, S. W., Lohani, T. N., & Kato, S. (2022). Characterizing Suction Stress and Shear Strength for Unsaturated Geomaterials under Various Confining Pressure Conditions. *Transportation Geotechnics*, 34, 100-747.
  15. Li, S., Yang, Z., Tian, X., Xiao, Y., Li, X., & Liu, X. (2021). Influencing factors of scale effects in large-scale direct shear tests of soil-rock mixtures based on particle breakage. *Transportation Geotechnics*, 31, 100-677.
  16. Liu, X., Degao, Z., Jingmao, L., Bowen, Z. (2021). Predicting the small strain shear modulus of coarse-grained soils. *Soil Dynamics and Earthquake Engineering* 141: 106-468.
  17. Mishra, P., & Khare, G. P. (2021). Investigation of the suction of peat soil in the drying and wetting process. *Materials Today: Proceedings*.
  18. Miao, H., & Wang, G. (2022). Shear rate effect on the residual strength of saturated clayey and granular soils under low-to high-rate continuous shearing. *Engineering Geology*, 308, 106-821.
  19. Moreira, E. B., Baldovino, J. A., Rose, J. L., & dos Santos Izzo, R. L. (2019). Effects of porosity, dry unit weight, cement content and void/cement ratio on unconfined compressive strength of roof tile waste-silty soil mixtures. *Journal of Rock Mechanics and Geotechnical Engineering*, 11(2), 369-378.
  20. Teramage, M. T., Carasco, L., & Coppin, F. (2019). Impact of drying and wetting cycles on 137Cs ageing in forest soils contaminated with different input forms. *Journal of environmental radioactivity*, 203, 93-97.
  21. Osinubi, K. J., Eberemu, A. O., Yohanna, P., & Azige, P. (2022). Reliability based predictive model for estimating shear strength values of locust bean waste ash compacted black cotton soil. *Cleaner Materials*, 5, 100114.
  22. Patle, K. S., Panchal, V., Saini, R., Agrawal, Y., & Palaparthi, V. S. (2022). Temperature compensated and soil density calibrated soil moisture profiling sensor with multi-sensing point for in-situ agriculture application. *Measurement*, 201, 111-703.
  23. Pan, L., Chen, Y., Xu, Y., Li, J., & Lu, H. (2022). A model for soil moisture content prediction based on the change in ultrasonic velocity and bulk density of tillage soil under alternating drying and wetting conditions. *Measurement*, 189, 110-504.
  24. Poncelet, N., & François, B. (2022). Effect of laboratory compaction mode, density and suction on the tensile strength of a lime-treated silty soil. *Transportation Geotechnics*, 34, 100763.
  25. Rajaram, G., & Erbach, D. C. (1998). Drying stress effect on mechanical behaviour of a clay-loam soil. *Soil and Tillage Research*, 49(1-2), 147-158.
  26. Rücknagel, J., Hofmann, B., Paul, R., Christen, O., & Hülsbergen, K. J. (2007). Estimating precompression stress of structured soils on the basis of aggregate density and dry bulk density. *Soil and Tillage Research*, 92(1-2), 213-220.
  27. Al Tarhouni, M. A., & Hawlader, B. (2021). Monotonic and cyclic behaviour of sand in direct simple shear test conditions considering low stresses. *Soil Dynamics and Earthquake Engineering*, 150, 106931.
  28. Ueno, K., Seiichiro, K., Toshikazu, H., Fumio, T. (2019). Elastic shear modulus variations during undrained cyclic loading and subsequent reconsolidation of saturated sandy soil. *Soil Dynamics and Earthquake Engineering* 116: 476 – 489,
  29. Xu, Y., Zeng, Z., & Lv, H. (2020). Comparative study on thermal properties of undisturbed and compacted lateritic soils subjected to drying and wetting. *Engineering Geology*, 277, 105-800.
  30. ZHAO, X. D., ZHOU, G. Q., & TIAN, Q. H. (2009). Study on the shear strength of deep reconstituted soils. *Mining Science and Technology (China)*, 19(3), 405-408.
  31. Yao, Y., Li, J., Ni, J., Liang, C., & Zhang, A. (2022). Effects of gravel content and shape on shear behaviour of soil-rock mixture: Experiment and DEM modelling. *Computers and Geotechnics*, 141, 104476.
  32. Yoon, S., Chang, S., & Park, D. (2022). Investigation of soil-water characteristic curves for compacted bentonite considering dry density. *Progress in Nuclear Energy*, 151, 104318.
  33. The Viet Nam Standard “TCVN 4195:2012” for Soils - Laboratory methods for determination of density.
  34. The Viet Nam Standard “TCVN 4199:1995” for Soil - Laboratory method of determination of shear resistance in a shear box apparatus.

**Copyright:** ©2023 Thy Truc Doan. This is an open-access article distributed under the terms of the Creative Commons Attribution License, which permits unrestricted use, distribution, and reproduction in any medium, provided the original author and source are credited.